



Contents lists available at ScienceDirect

Corrosion Science

journal homepage: www.elsevier.com/locate/corsci



Towards a reliable determination of the intergranular corrosion rate of austenitic stainless steel in oxidizing media

B. Gwinner^{a,*}, M. Auroy^a, F. Balbaud-Célrier^b, P. Fauvet^c, N. Larabi-Gruet^a,
P. Laghoutaris^a, R. Robin^a

^a CEA, DEN, DANS, DPC, SCCME, Laboratoire d'Etude de la Corrosion Non Aqueuse, F-91191 Gif-sur-Yvette, France

^b CEA, DEN, Direction de l'Assainissement et du Démantèlement Nucléaire, F-91191 Gif-sur-Yvette, France

^c CEA, DEN, DANS, DPC, Service d'Etude de la Corrosion et du Comportement des Matériaux dans leur Environnement, F-91191 Gif-sur-Yvette, France

ARTICLE INFO

Article history:

Received 10 September 2015

Received in revised form 4 February 2016

Accepted 12 February 2016

Available online xxx

Keywords:

A. Stainless steel

B. Modelling studies

B. Weight loss

C. Acid corrosion

C. Intergranular corrosion

C. Transpassivity

ABSTRACT

This paper studies the corrosion behaviour of non-sensitized stainless steels in oxidizing environments, where they can suffer intergranular corrosion. In this case, corrosion rate estimated by gravimetric measurement is not constant as a function of time. This paper proposes a quantitative modelling of the IGC kinetics. Two models were developed: the first one is based on the geometrical simulation of the groove penetration; the second one uses a semi-empirical approach based on the typical shape of the corrosion kinetics. Both models reproduce successfully the experimental corrosion kinetics observed for a AISI 310L stainless steel corroded in nitric acid containing oxidizing ions.

© 2016 Elsevier Ltd. All rights reserved.

1. Introduction

Austenitic stainless steels (SS) can be prone to intergranular corrosion (IGC) in oxidizing medium such as nitric acid. IGC is characterized by a preferential attack at grain boundaries, which induces an acceleration of the SS degradation. Two cases of IGC can be distinguished depending on the corrosion mechanism that is involved [2,3]. The first case of IGC concerns the austenitic SS which contain precipitates. This is most specifically the case of sensitized SS (induced by tempering during welding, for example) where chromium carbides of $M_{23}C_6$ type are formed at grain boundaries in the heat affected zones [4–21]. During tempering, the formation of these chromium carbides and the relative slow diffusion of chromium in the matrix induce the formation of adjacent chromium depleted zones [16,19]. Due to their lower corrosion resistance, these chromium depleted zones are preferentially attacked by the medium. This process is probably worsened by a galvanic coupling between the depleted zone and the more noble adjacent zones [14]. Note that in oxidizing medium such as nitric acid, chromium carbides can also be themselves attacked by

nitric acid. The resulting IGC morphology has a quite disordered aspect (Fig. 1, left). Grains drop more or less and the SS is non-uniformly affected in terms of depth. This quite heterogeneous IGC can be related to the spatial distribution of the chromium carbides in SS and more specifically to their connection degree [18,19]. The repartition of chromium carbides is mainly dependant on the tempering conditions [8–10,13,16,20]. On an electrochemical point of view, the presence of chromium depleted zones has consequences on the anodic behaviour of the stainless steel (Fig. 2). The global anodic current is increased on the overall anodic domain, mostly due to the contribution of the chromium depleted zones. It is therefore highlighted that the IGC sensitiveness is present whatever the oxidizing character of the medium is. Therefore different experimental tests are classically performed to study this IGC case namely weight-loss techniques called “Huey”, “Streicher” or “Strauss” tests (ASTM A 262) or electrochemical techniques such as single-loop or double-loop electrochemical potentiokinetic reactivation (SL-EPR or DL-EPR) [4–6,8,13,17–20].

The second case of IGC is related to austenitic stainless steels which do not contain any precipitate [27]. It is particularly the case of low carbon content SS which are solution-annealed and quenched. In this case, IGC can also be present but only in a very oxidizing medium [28,29]. In such an oxidizing medium, SS is polarized in its transpassive domain, in which the SS is no more protected

* Corresponding author.

E-mail address: benoit.gwinner@cea.fr (B. Gwinner).

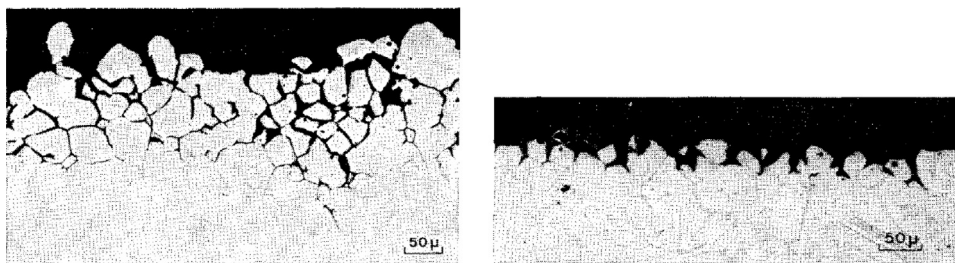


Fig. 1. Examples of IGC morphology for a sensitized SS (left—AISI 304 SS (C = 0.034 wt.%) tempered 30 min at 700 °C and corroded in boiling HNO₃ 14 mol/L during 240 h) and a non-sensitized SS (right—AISI 310L SS corroded in boiling HNO₃ 13 mol/L during 50 h with Au coupling) [22].

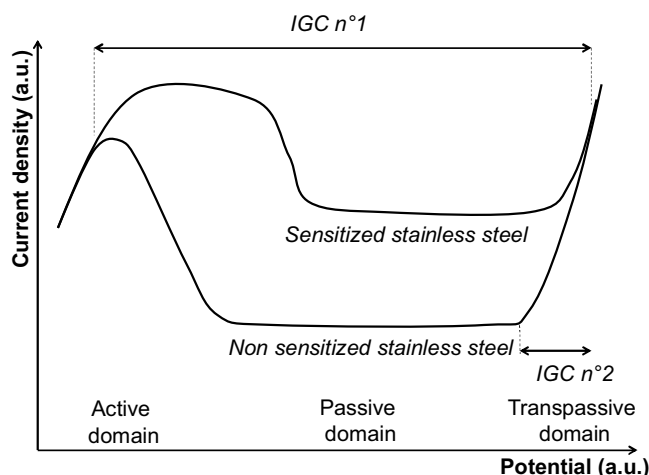


Fig. 2. Schematic illustration of the SS anodic behaviour and the potential range of sensitivity to IGC for a sensitized and a non-sensitized SS [19,23–26].

by a passive film (Fig. 2) [30]. IGC is characterized by the formation of triangular grooves at grain boundaries. The progression of grooves leads to grain dropping with a certain periodicity. Despite the localized nature of IGC, the morphology of this kind of IGC is characterized by a quite ordered geometry covering the whole surface (Fig. 1, right). The origin of this kind of IGC seems to be not universally explained. On the one hand, the specific reactivity of grain boundaries is attributed to chemical reasons (associated with the presence of segregations at grain boundaries) [24,31–33]. It is shown that both phosphorus [23,25,30,34–43] and silicon [3,23,25,37–41,43–62] have an impact on the occurrence and kinetics of IGC. These conclusions motivate some authors to produce SS with optimized impurities content [43,63–68]. On the other hand, the specific reactivity of grain boundaries is explained by the particular metallurgy of grain boundaries [3,18,23,31,32,69]. It is shown that the grain boundary structure, especially the relative misorientation of adjacent grains, impacts the kinetics of grain boundary attack. Despite of the relatively ordered character of this second kind of corrosion, the consequences of IGC on the SS seem not to be clearly understood in a quantitative point of view. For example the accelerating mass loss observed for a material corroded by IGC is attributed by some authors to the grain dropping and by some others to the increase of the surface in contact with the media [70]. To answer to this question, only few attempts were made to quantify the IGC kinetics. Some of them are based on the measurement of grooves depth only [70–74]. Some others describe more precisely the morphology of grooves in terms of width and depth [75]. Recently, a very promising approach based on cellular automata was proposed to simulate the evolution of IGC as a function of time [36,76]. This method consists in discretizing the SS/medium system into a regular grid of cells (with a cubic or rhombic dodecahedron geometry, for example). Three different cells are defined: interior

Table 1

chemical composition of AISI 310L SS.

Element	Fe	C	Cr	Ni	Mn	Si	P	S	Mo	Nb
wt.%	bal.	0.006	24.32	21.13	1.03	0.13	0.016	0.001	0.08	0.115

of grain (bulk) cells, grain boundary cells and medium cells. The progressive dissolution of bulk cells and grain boundary cells is simulated by changing them into medium cells, when they are in contact with medium cells.

But in our opinion, all these attempts do not describe sufficiently precisely the IGC kinetics. The main aim of this work is to propose some clarifications in this domain and more precisely to give tools to extrapolate quantitatively the IGC kinetics obtained experimentally in short duration. For that purpose, two distinct models are proposed: a geometrical model based on a morphological approach and a semi-empirical model based on the exploitation of the mass loss evolution as a function of time. In the first part of this paper, an IGC experiment was performed so as to give an experimental reference for both models. In the following two parts, the theoretical bases of both models are successively described and simulations are compared with the experimental data. In the last part, an example of application of both models is given to assess their interest and their accuracy.

2. Experimental setup

The corrosion test was performed on an AISI 310L stainless steel (commercial name “Uranus 65”) provided by Creusot Loire Industrie. This stainless steel has a low carbon content and was solution annealed (at 1100 °C during 30 min) and quenched, avoiding the formation of carbides which would lead to another kind of IGC. The chemical composition and the microstructure are given in Table 1 and Fig. 3, respectively. The mean grain size (84 μm) was determined using the normalized NF EN ISO 643:2003.

The corrosion medium was 8 mol/L nitric acid at boiling temperature (at this concentration the boiling temperature of nitric acid is 111 °C) containing 200 mg/L of vanadium(V) (introduced as 357 mg/L of V₂O₅). With the use of such an oxidizing medium ($E^{\circ}(\text{NO}_3^-/\text{HNO}_2) = 0.934 \text{ mV/SHE}$ and $E^{\circ}(\text{VO}_2^+/\text{VO}^{++}) = 1.004 \text{ V/SHE}$), it was expected that the corrosion potential of the stainless steel would shift towards the transpassive domain where IGC appears [3,77]. This corrosion medium was renewed after each corrosion period (160 h). The corrosion test was performed until the IGC steady-state was reached. The chemical stability of this medium was controlled periodically with acid-base titration (with 1 mol/L NaOH) and by UV–vis spectroscopy (Carry 50 model from Varian). This latter was used to verify that no reduction of vanadium(V) into vanadium(IV) occurred (VO²⁺ absorbance at 740 nm). Moreover the corrosion (on a Uranus 65 electrode) and redox (on a platinum electrode) potentials were continuously measured during the corrosion test. An example of measurement

Download English Version:

<https://daneshyari.com/en/article/7894467>

Download Persian Version:

<https://daneshyari.com/article/7894467>

[Daneshyari.com](https://daneshyari.com)